Los canales iónicos son proteínas que tienen un poro

Generalmente son muy selectivos: solo iones específicos pueden atravesar el poro de cada tipo de canal.
Los canales iónicos cambian su conformación dependiendo de varios factores. Estos cambios conformacionales permiten que cambien entre estados abiertos (poro accesible) o cerrados. Cuando están abiertos los iones específicos pueden fluir de un lado al otro del canal de acuerdo a la fuerza electroquímica que sienten (gradiente de concentración y campo eléctrico).

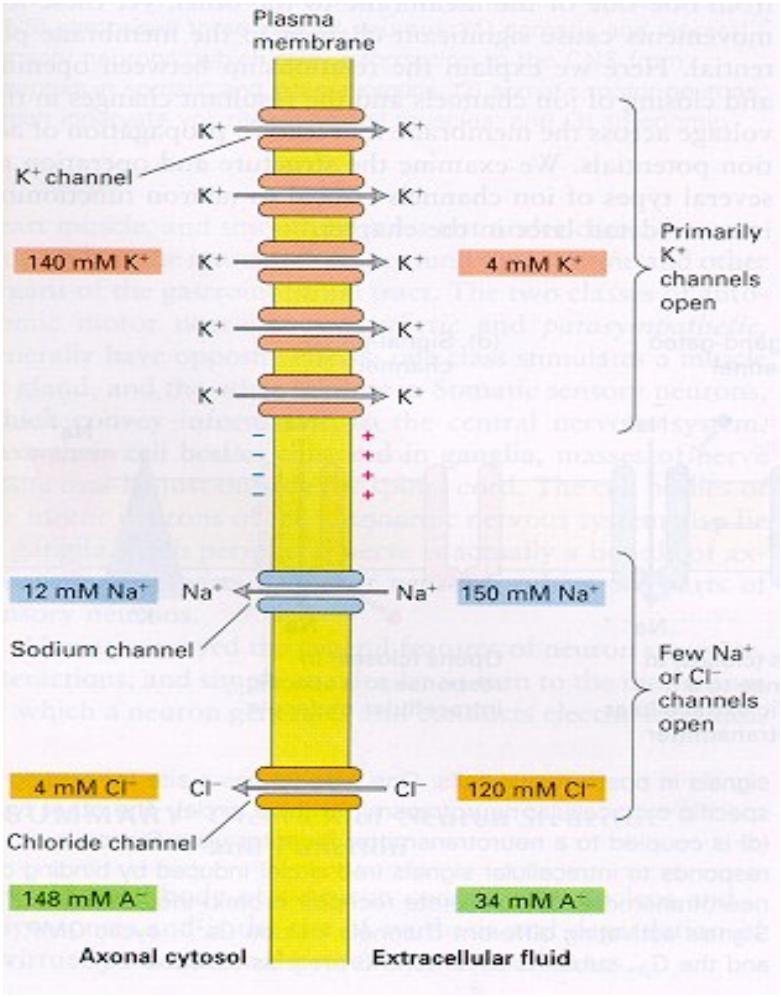

Los canales voltaje-dependientes cambian de conformación cuando cambia el potencial de membrana.
Los ligando-dependientes cambian su conformación cuando ligan alguna sustancia (ligandos).

Pueden ser estudiados con métodos electrofisiológicos (ya que la corriente iónica puede ser medida).

Voltage clamp technique

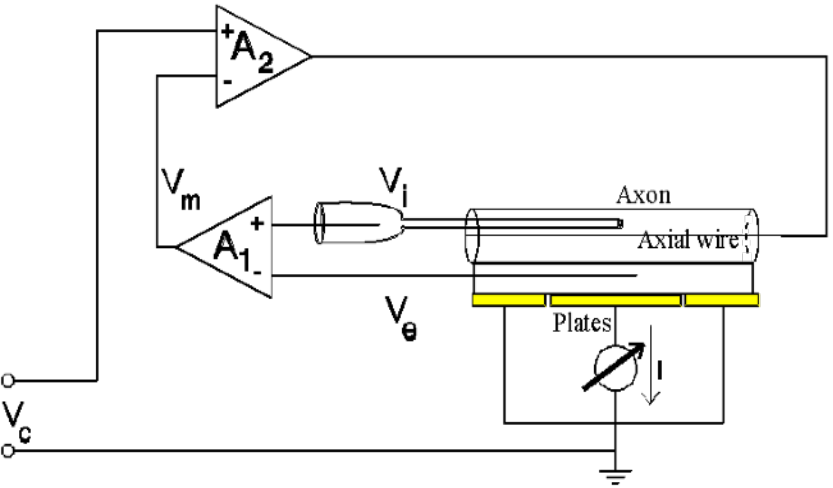

Figure 18. Voltage clamp of the squid giant axon. V_i is the internal potential measured with a pipette inserted in the axon. V_e is the external potential measured by an external electrode. $V_m = V_i - V_e$, as computed by amplifier A_1. A_2 compares V_m with V_c (which is the command voltage) to inject current I, which maintains V_m at V_c. The current is injected by the axial wire and crosses the axon membrane and is drained by the chamber plates and measured by a current measuring device..

(Figuras de F. Bezanilla)

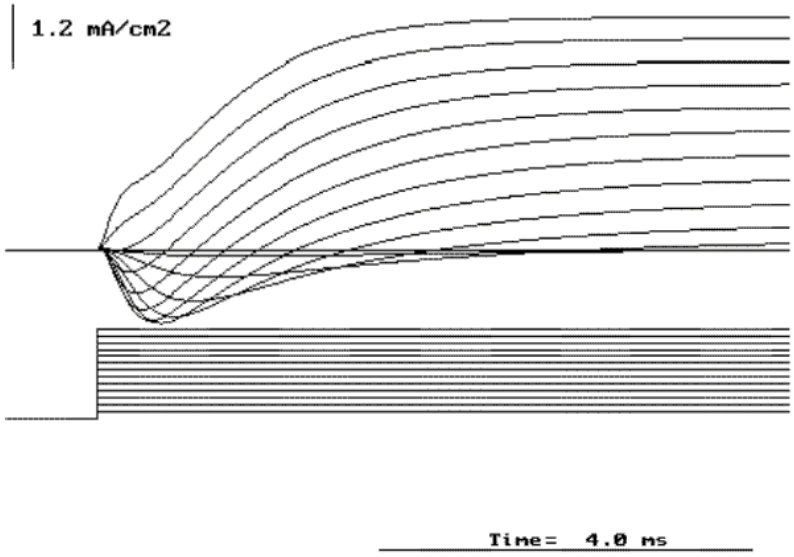

Currents in response to depolarizing pulses from -60 to 60 mV in increment of 10 mV from a holding potential of -70 mV.

El estudio de los canales cambió muchísimo con la introducción de la técnica de patch-clamp (Neher y Sackman).

Patch clamp.

Permite medir la corriente a través de uno o unos pocos canales. Para eso se usa una pipeta delgada que genera un sello que ofrece una enorme resistencia al flujo hacia los costados. Hay distintas configuraciones

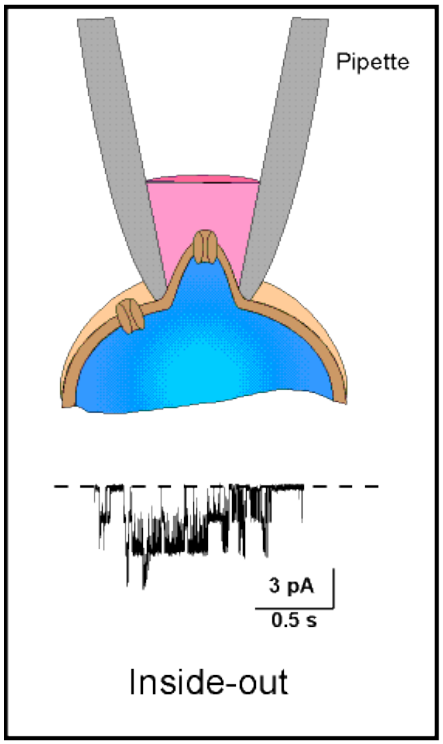

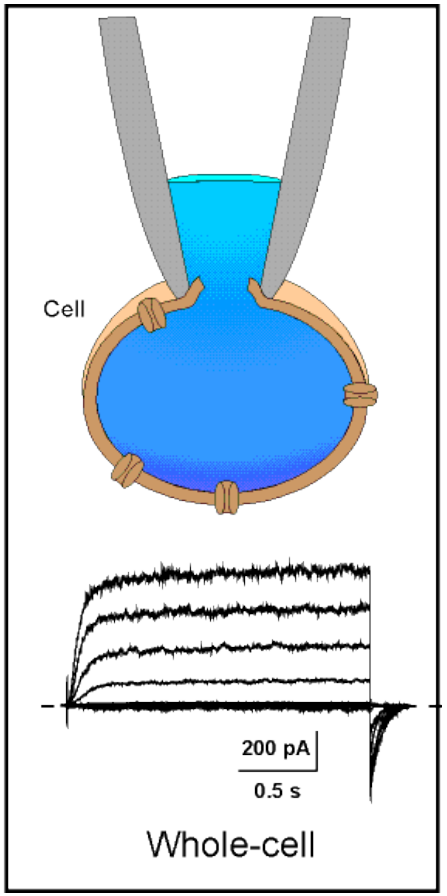

Dependiendo de la configuración, la corriente medida puede corresponder a la que atraviesa a uno o pocos canales (inside-out configuration) o a todos los canales de la membrana (whole-cell configuration). La línea punteada corresponde a corriente cero.

A partir de los experimentos de canal único es posible calcular la probabilidad de apertura en el estado estacionario (se calcula como el cociente entre el tiempo durante el cual el canal permanece abierto dividido por el tiempo total de la observación).

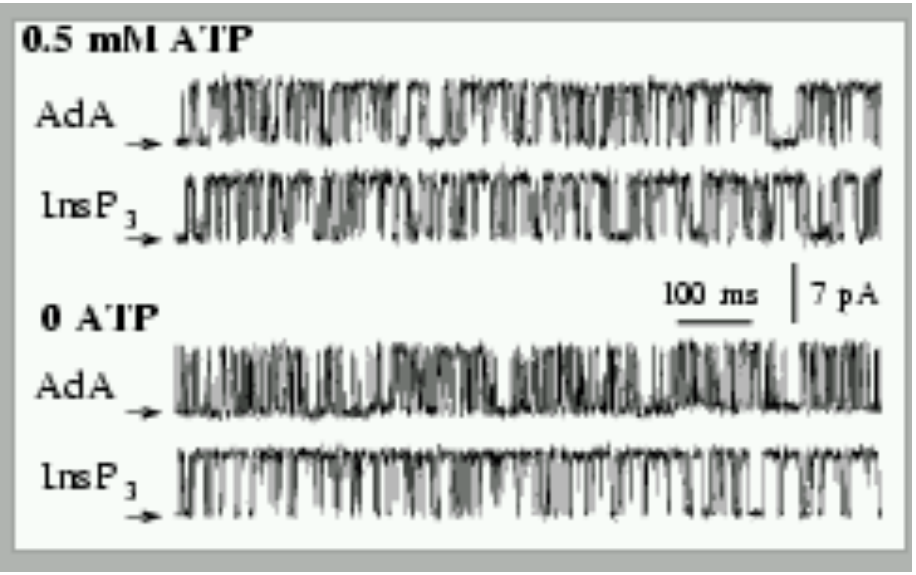

Single channel records

Probabilidad de apertura

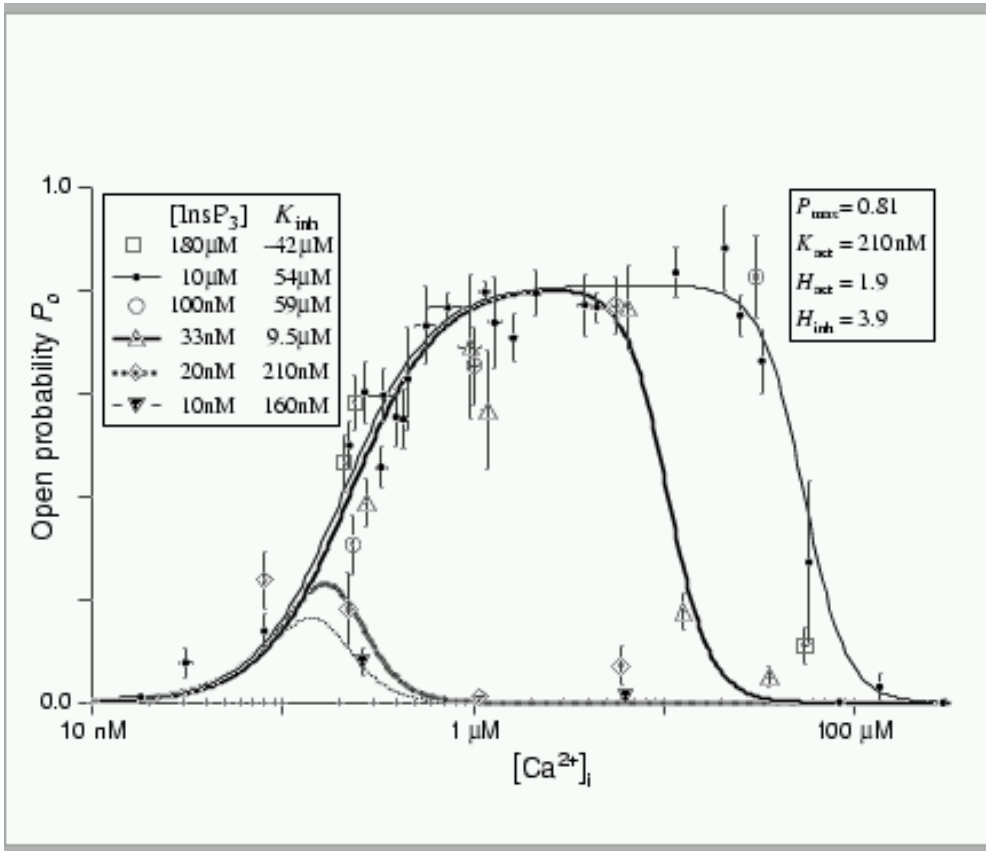

Figures provided by D Mak and K Foskett

A canal de K+

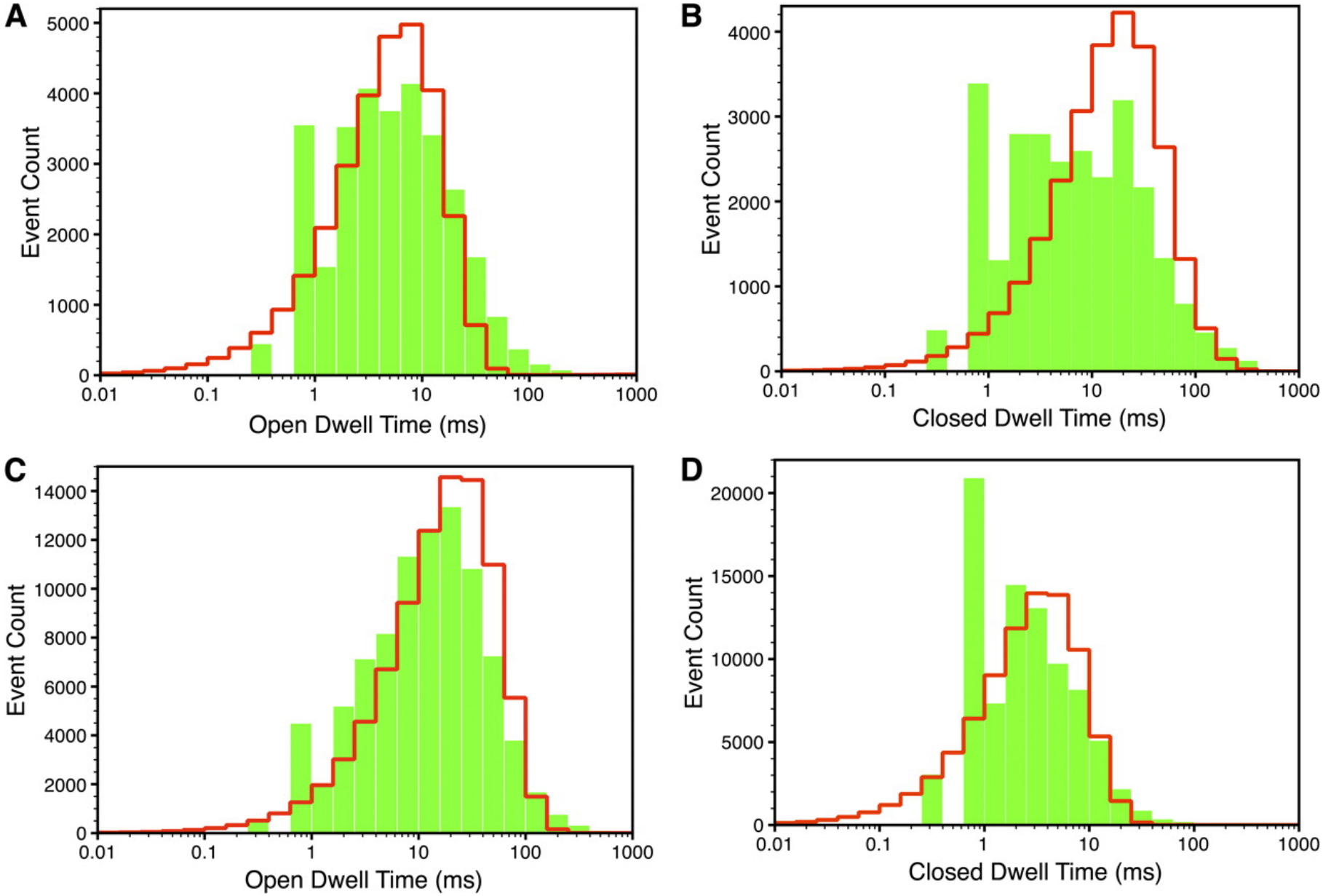

Se pueden calcular las “dwell time distributions” (distribución de tiempos de espera)

A partir de las observaciones se pueden construir modelos cinéticos (Hidden Markov Models). Problema: muchas topologías equivalentes entre sí!!

Existen también técnicas de visualización y preparación que permiten ver otros procesos estocásticos que ocurren en células (que se solían estudiar en términos de una descripción de "campo medio").

Ever-fluctuating single enzyme molecules: Michaelis-Menten equation revisited

Brian P English[1], Wei Min[1], Antoine M van Oijen[1,4], Kang Taek Lee[1,4], Guobin Luo[1], Hongye Sun[1,4], Binny J Cherayil[1,2], S C Kou[3] & X Sunney Xie[1]

Enzymes are biological catalysts vital to life processes and have attracted century-long investigation. The classic Michaelis-Menten mechanism provides a highly satisfactory description of catalytic activities for large ensembles of enzyme molecules. Here we tested the Michaelis-Menten equation at the single-molecule level. We monitored long time traces of enzymatic turnovers for individual β-galactosidase molecules by detecting one fluorescent product at a time. A molecular memory phenomenon arises at high substrate concentrations, characterized by clusters of turnover events separated by periods of low activity. Such memory lasts for decades of timescales ranging from milliseconds to seconds owing to the presence of interconverting conformers with broadly distributed lifetimes. We proved that the Michaelis-Menten equation still holds even for a fluctuating single enzyme, but bears a different microscopic interpretation.

NATURE CHEMICAL BIOLOGY VOLUME 2 NUMBER 2 FEBRUARY 2006

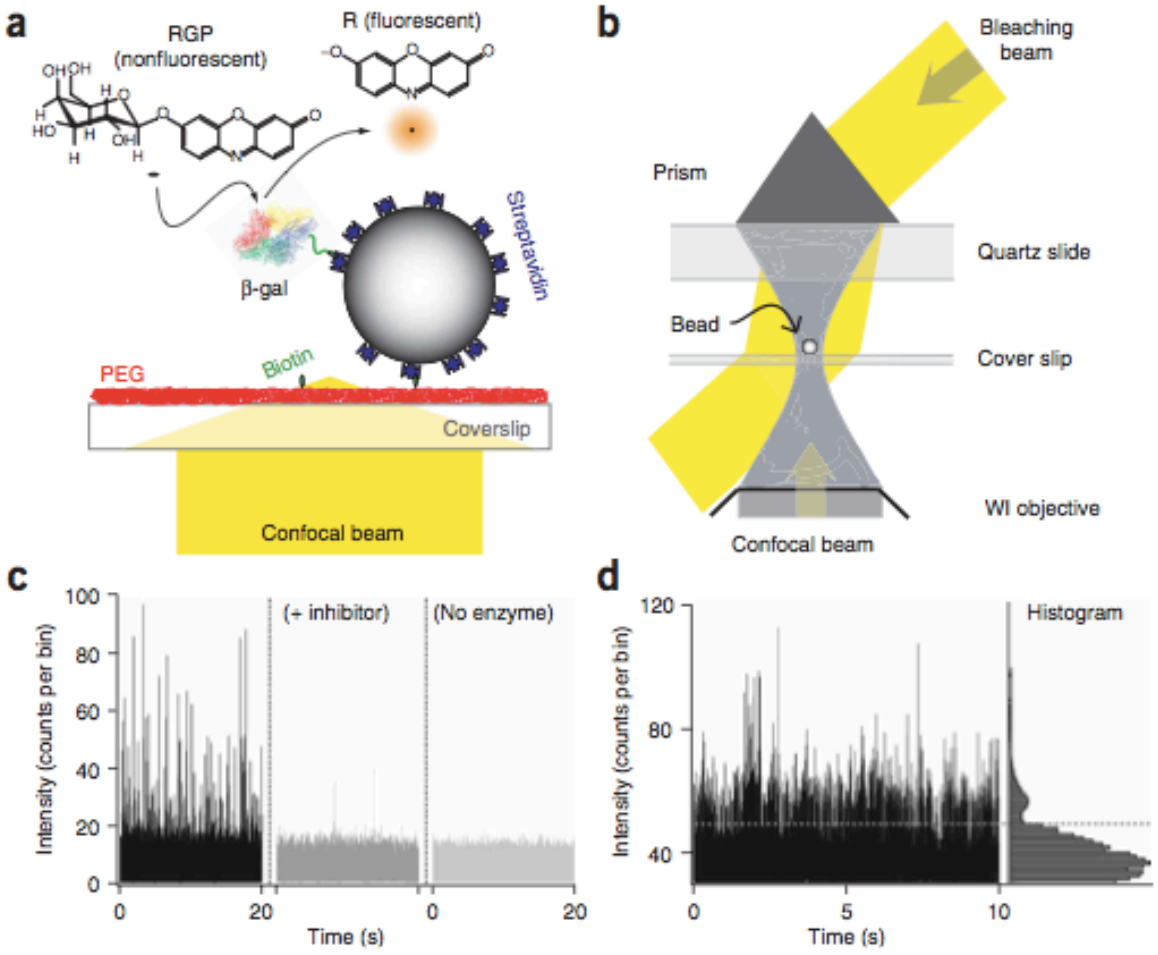

Figure 1 Single-molecule assay with fluorescent product. (**a**) Schematic representation of enzyme immobilization (not to scale). A single β-galactosidase molecule is linked to a streptavidin-coated polystyrene bead through a flexible PEG linker. The bead binds to the hydrophilic biotin-PEG surface of the glass coverslip. A photogenic resorufin-β-D-galactopyranoside (RGP, **1**) substrate in buffer solution is converted to a fluorescent resorufin (R, **2**) product by the single enzyme molecule, and detected one molecule at a time before it rapidly diffuses out of the confocal detection volume. (**b**) Schematic representation of the photobleaching and detection beams. A lens focuses a 550-mW, 560-nm photobleaching beam to a 200-μm-diameter spot surrounding the bead. The beam is coupled into the 100-μm-thick flow cell by a prism atop the quartz slide. The water immersion (WI) objective is used to focus a 1-mW, 560-nm detection beam onto a diffraction-limited spot around the bead and to collect the emission for detection with a photon-counting avalanche photodiode detector. (**c**) Turnover time trace of a single β-galactosidase molecule at 20 μM RGP. Left, fluorescence intensity as a function of time for a β-galactosidase molecule undergoing enzymatic turnovers, each giving a fluorescence burst. Middle, data for the same enzyme molecule after addition of 200 μM PETG inhibitor. Right, data for a bead without enzyme (no inhibitor). All time traces are obtained with 0.5-ms time bins. (**d**) Turnover time traces of a single β-galactosidase molecule at 100 μM RGP. Dashed line represents the threshold used to determine waiting times between two adjacent burst (see **Supplementary Methods** and **Supplementary Fig. 1** online). The intensity histogram of the enzymatic time trace is shown at right. The time trace has 0.5-ms time bins.

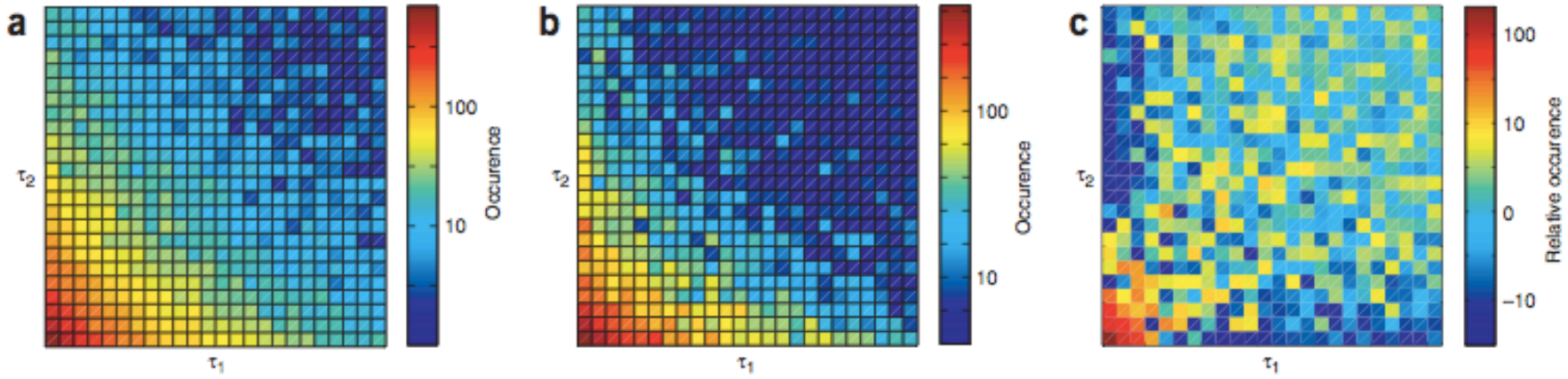

Figure 4 Two-dimensional joint-probability distributions of waiting times. (**a**) The 2D joint probability distribution of two adjacent waiting times (τ_1 and τ_2), $g(\tau_1,\tau_2)$, obtained from the time trace of a single β-galactosidase molecule at 100 μM substrate concentration. The τ_1 and τ_2 axes run from 0 to 12 ms. The color code represents the occurrence (*z* axis) from 500 (deep red) to 1 (dark blue). (**b**) The 2D joint probability distribution of two waiting times (τ_1 and τ_2) at a larger separation for same time trace as in **a**, which can be represented by $f(\tau_1)f(\tau_2)$ because of the lack of correlation between τ_1 and τ_2. The time axes are the same as in **a**. (**c**) The difference 2D histogram, $\delta(\tau_1, \tau_2) = g(\tau_1, \tau_2) - f(\tau_1)\, f(\tau_2)$. The time axes are the same as in **a**. The pixels in 'cold' colors (less probable) gather along two wings in the *x*-*y* plot, whereas those with 'warm' color (more probable) are mainly spread around the diagonal. A long waiting time tends to be followed by a long one, and a short waiting time tends to be followed by a short one.

Distintos métodos para estudiar canales

Funcionales

- Current clamp *(record membrane potential)*
- Voltage clamp *(record ionic currents)*
  - Macroscopic
    - 2-electrode
    - Whole-cell patch clamp
  - Microscopic (single channels)
    - Cell-attached
    - Inside-out
    - Outside-out
- Gating current
- Spectroscopy

Estructurales

- Biochemistry
- Molecular biology
- Structural (x-ray, etc.)

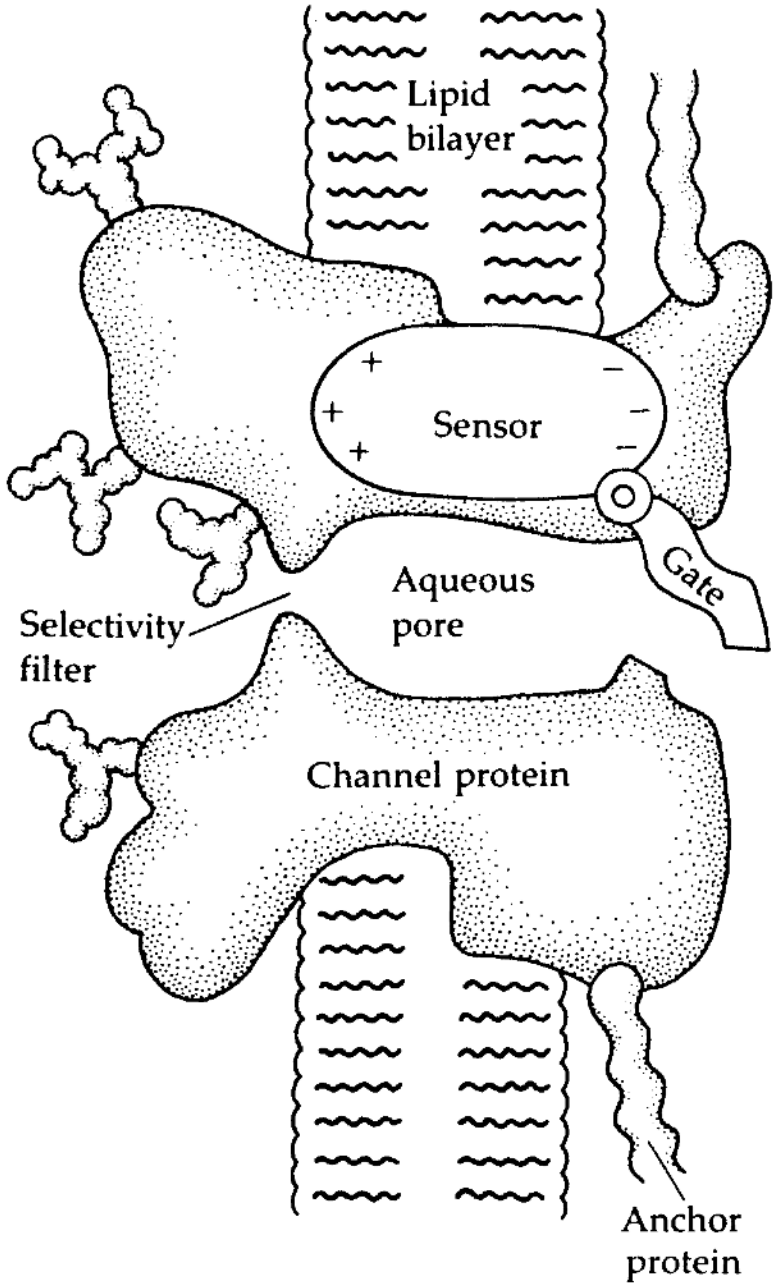

¿Cómo es la estructura del canal?

Ejemplo: canal de K+ voltaje dependiente

Hille (1984)

3 WORKING HYPOTHESIS FOR A CHANNEL

The channel is drawn as a transmembrane macromolecule with a hole through the center. The external surface of the molecule is glycosylated. The functional regions, selectivity filter, gate, and sensor are deduced from voltage-clamp experiments but have not yet been charted by structural studies. We have yet to learn how they actually look.

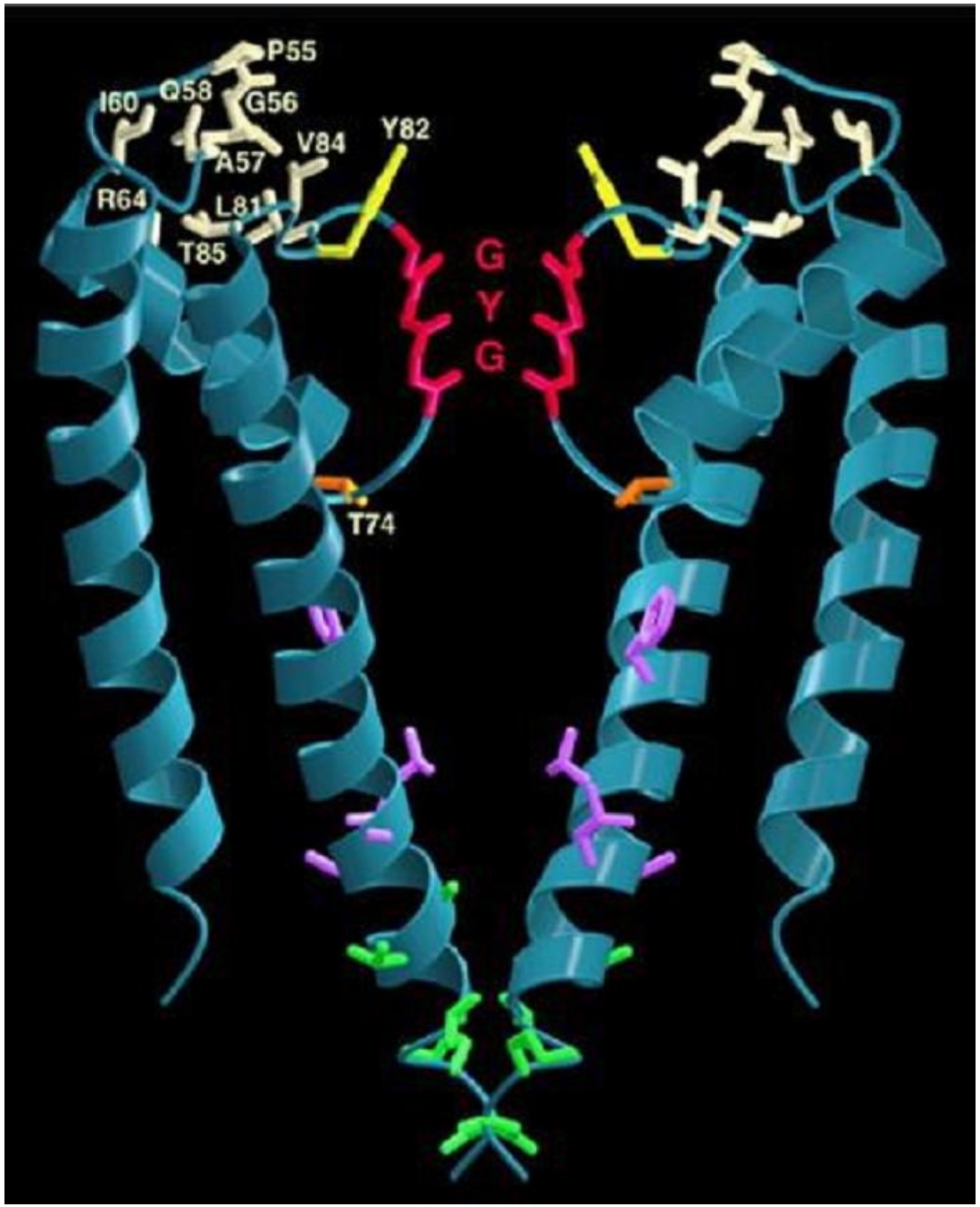

Bacterial K^+ channel
X-ray crystallography

← Selectivity filter

← Inner vestibule

← Gate

Estructura de un canal de K+, Science 1998

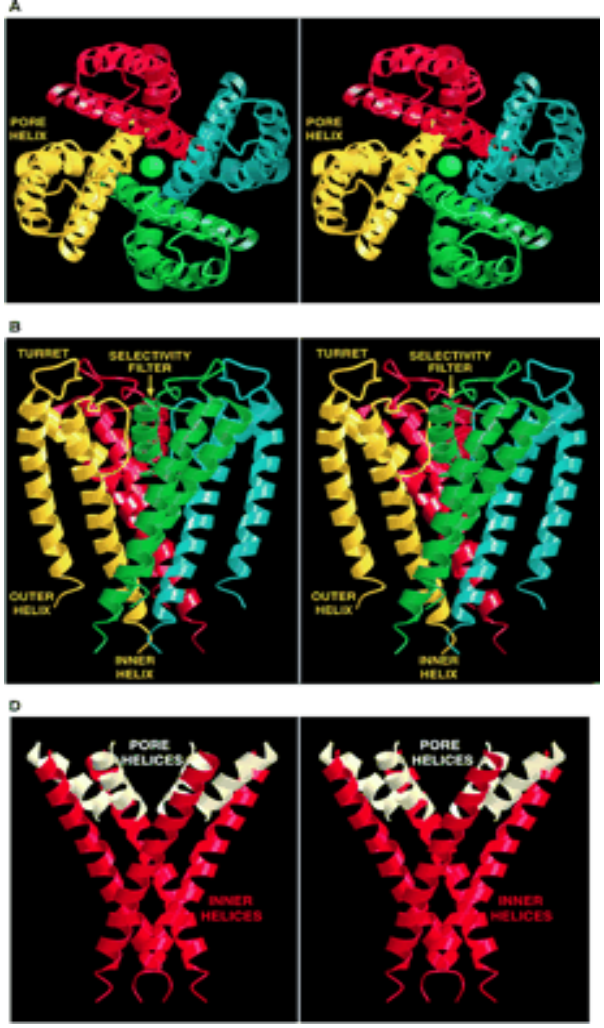

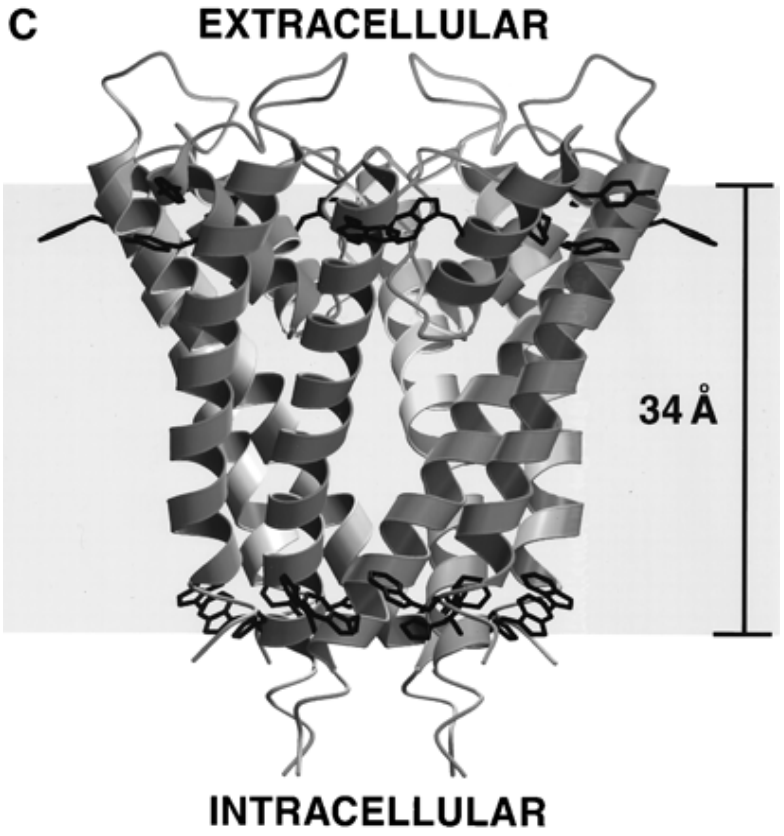

Views of the tetramer**.** (**A**) Stereoview of a ribbon representation illustrating the three-dimensional fold of the KcsA tetramer viewed from the extracellular side. The four subunits are distinguished by color. (**B**) Stereoview from another perspective, perpendicular to that in (A). (**C**) Ribbon representation of the tetramer as an integral-membrane protein. Aromatic amino acids on the membrane-facing surface are displayed in black. (**D**) Inverted teepee architecture of the tetramer.

Energetics of ion conduction through the K+ channel, Nature 2001

The crystallographic structure of the KcsA K^+ channel revealed that the pore comprises a wide, nonpolar cavity of 8 Å radius on the intracellular side, leading up on the extracellular side to a narrow pore of 12 Å that is lined exclusively by main chain carbonyl oxygens. This region of the pore acts as a 'selectivity filter' by allowing only the passage of K^+ ions across the cell membrane, whereas the wide cavity helps overcome the dielectric barrier caused by the cell membrane. The translocation of K^+ ions in single file through the narrowest region of the pore is expected to be the rate-limiting step in the conduction mechanism.

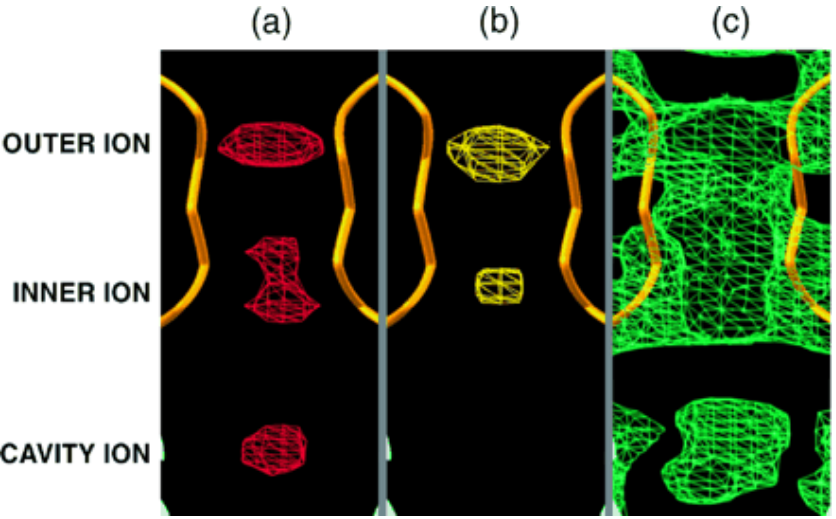

Identification of permeant ion positions in the pore.

Figuras de Science, 1998

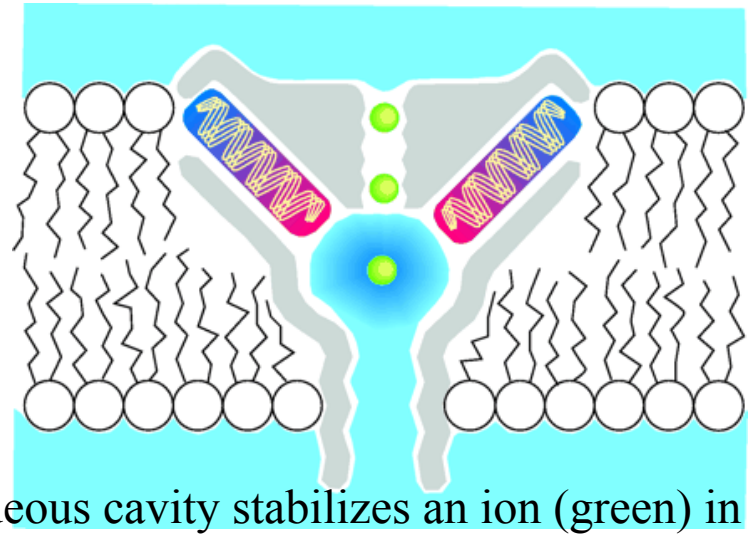

A large aqueous cavity stabilizes an ion (green) in the membrane interior andoriented helices point their partial negative charge towards the cavity where a cation is located.

Resultados de simulaciones de dinamica molecular

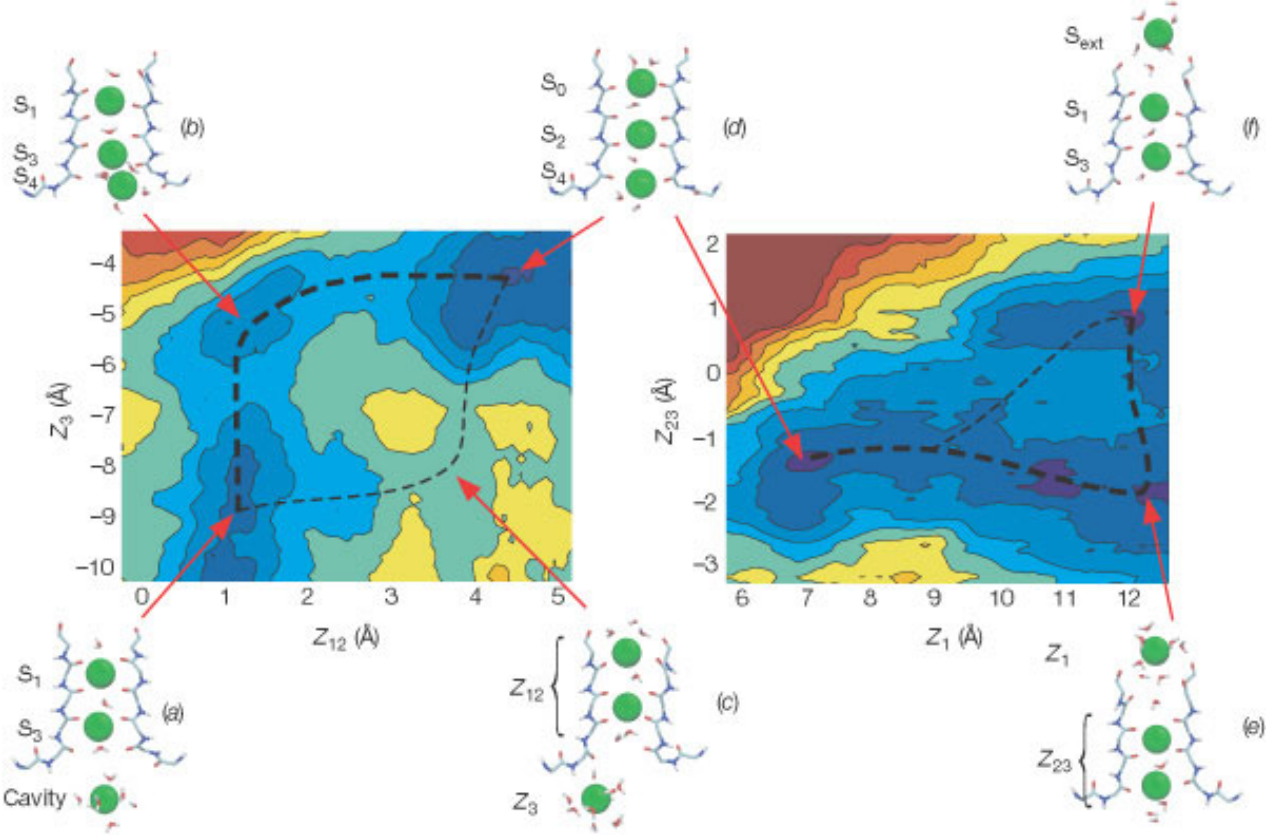

Topographic free energy maps of ion conduction. Each colour level corresponds to an energy of 1 kcal mol^{-1}; the axes are in Å. To produce the two-dimensional maps, the full free energy function $W(Z_1,Z_2,Z_3)$, which depends on the position of the three ions along the channel axis, has been projected onto two different planes with reduced reaction coordinates. Left: shown as a function of the position of the ion in the cavity, Z_3, and the position of the centre-of-mass of the two ions in the selectivity filter, Z_{12}. Right: shown as a function of the position of the outermost ion near the extracellular end of the pore, Z_1, and the position of the centre-of-mass of the two ions in the selectivity filter, Z_{23}

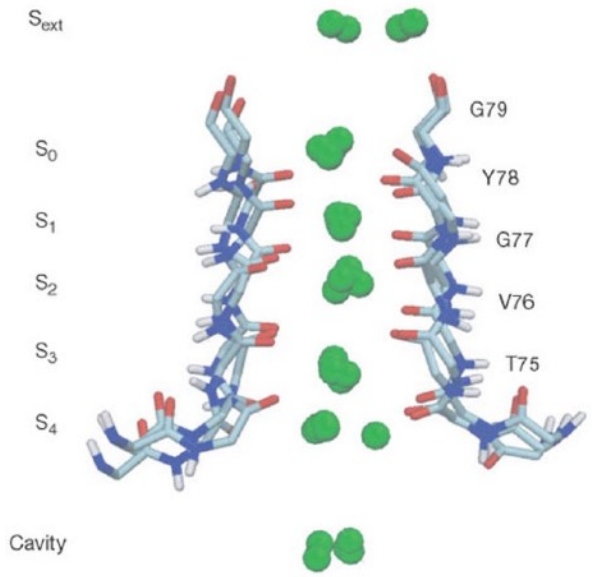

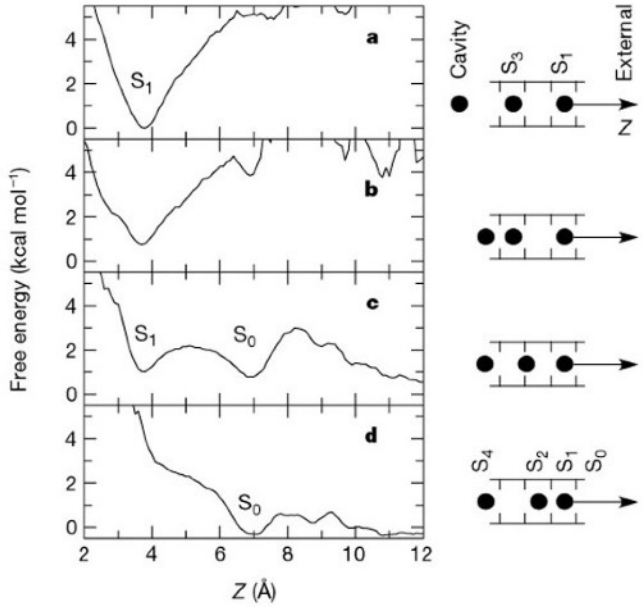

Even though no large free energy barrier opposing ion conduction is observed, some positions along the permeation pathway are preferably occupied by K^+ ions. Left: superposition of a few dynamical configurations associated with the free energy minima in the two dimensional maps. Five specific sites in the selectivity filter are revealed by the superposition. Right: free energy profile as a function of the position of the outermost ion while the two other ions are fixed at different locations in the pore. (a) The outer K^+ ion cannot exit towards the extracellular side while the other 2 ions are in the cavity and in the inner site S_3. As the ion in the cavity approaches the inner site S_4 and the second ion initiates a transition from site S_3 to S_2, the bottom of the free energy well is lifted up, thereby decreasing the barrier between sites S_1 and S_0. Ultimately, the site S_1 becomes unstable and the exit of the ion towards the extracellular side becomes barrierless (d). This demonstrates the importance of ion repulsion for permeation.

Referencias:

S. BERNÈCHE AND B. ROUX, "Energetics of ion conduction through the K^+ channel", *Nature* **414**, 73 - 77 (2001);
Declan A. Doyle, João Morais Cabral, Richard A. Pfuetzner, Anling Kuo, Jacqueline M. Gulbis, Steven L. Cohen, Brian T. Chait, Roderick MacKinnon, "The Structure of the Potassium Channel: Molecular Basis of K^+ Conduction and Selectivity", *Science* **280**, 69-77 (1998).

Zhou et al, Nature **414**, 43 (2001)
Cabral et al Nature **414**, 37 (2001)

Structural model of each of the four identical subunits of a voltage- gated K^+ channel

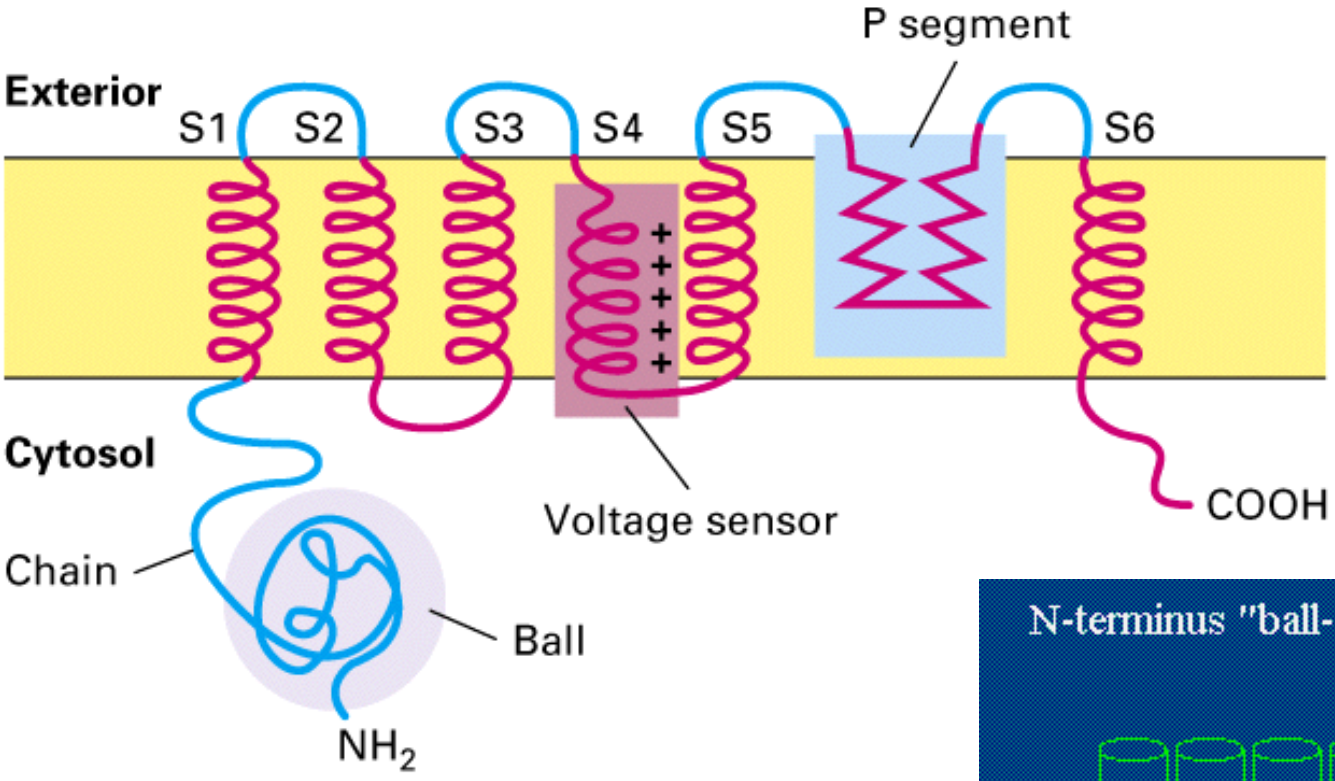

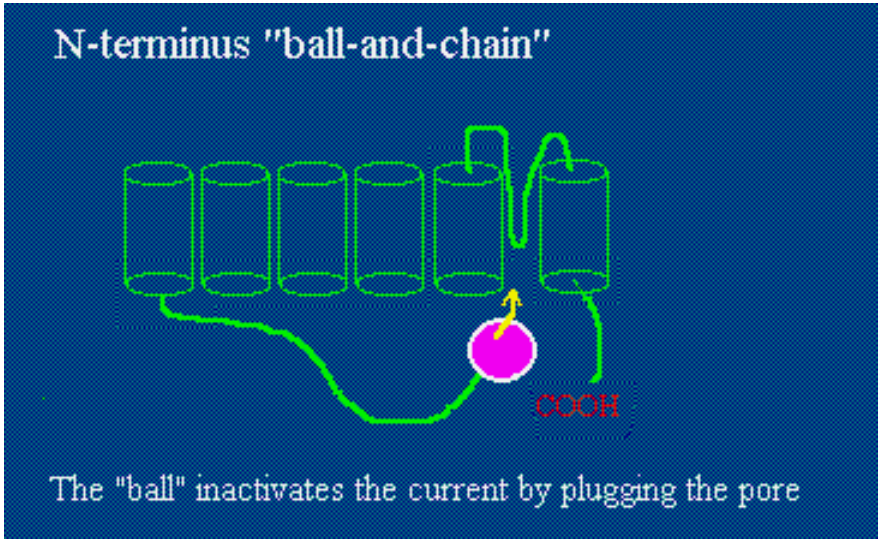

Open channel block

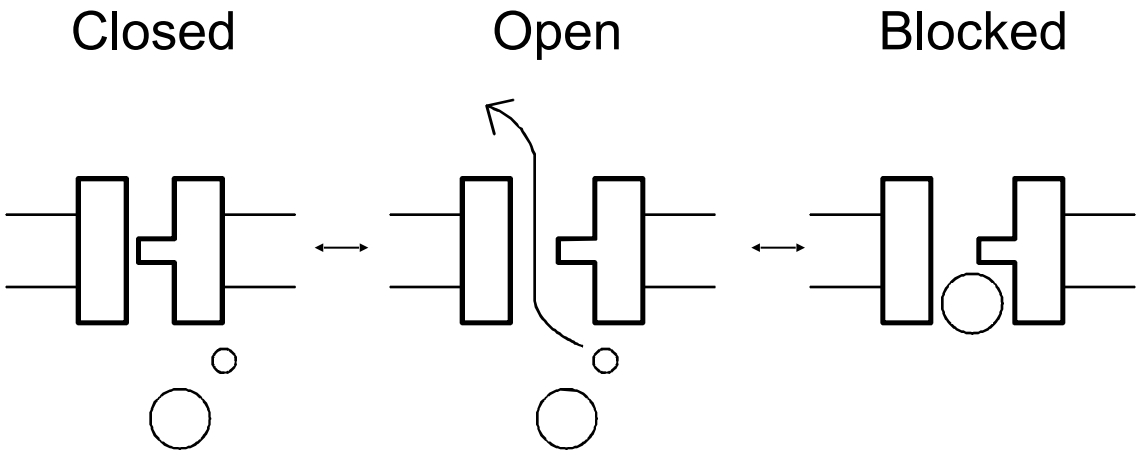

$$C \rightleftharpoons O \rightleftharpoons B$$
$$\Downarrow$$
$$OB$$

Ball-and-chain model for inactivation

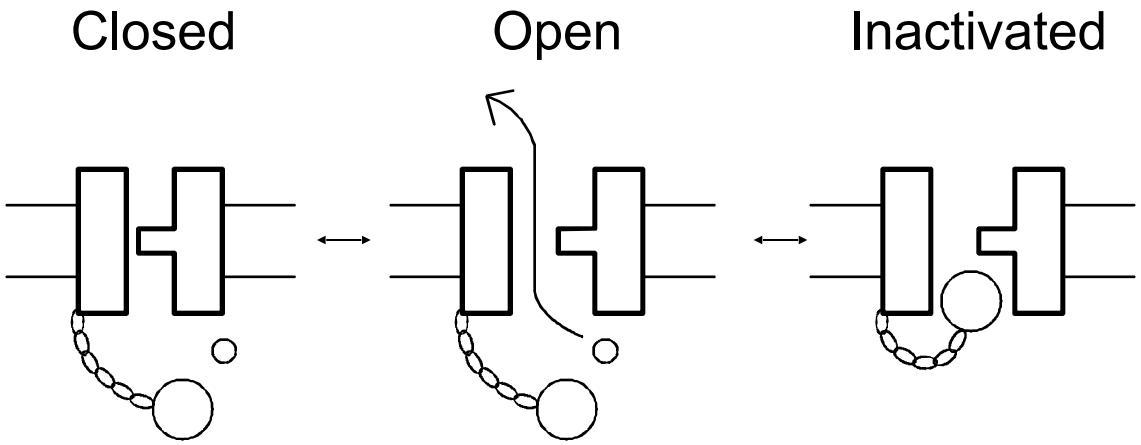

$$C \rightleftharpoons O$$
$$\Downarrow$$
$$I$$